

# GaSb and InP-based VCSELs at 2.3 $\mu\text{m}$ emission wavelength for tuneable diode laser spectroscopy of carbon monoxide

M. Ortsiefer\*<sup>a</sup>, C. Neumeyr<sup>a</sup>, J. Roskopf<sup>a</sup>, S. Arafin<sup>b</sup>, G. Böhm<sup>b</sup>, A. Hangauer<sup>c</sup>, J. Chen<sup>c</sup>,  
R. Strzoda<sup>c</sup>, M.-C. Amann<sup>b</sup>

<sup>a</sup>VERTILAS GmbH, Lichtenbergstr. 8, D-85748 Garching, Germany;

<sup>b</sup>Walter Schottky Institut, Am Coulombwall 3, D-85748 Garching, Germany;

<sup>c</sup>SIEMENS AG, Corporate Technology, Power & Sensor Systems, Otto-Hahn-Ring 6,  
D-81739 München, Germany

## ABSTRACT

We present long-wavelength buried tunnel junction (BTJ) VCSELs for emission wavelengths around 2.3  $\mu\text{m}$ . Two different device concepts have been realized utilizing either InP- or GaSb-based materials. The InP-VCSELs are based on a BTJ-design which has been well-proven for wavelengths up to 2  $\mu\text{m}$  in recent years. To extend this range up to emission wavelengths around 2.3  $\mu\text{m}$ , the main focus is set on an optimization of the active region. In this context, we use a graded and heavily strained quantum well design in conjunction with optimized growth conditions. The photoluminescence and x-ray characterization shows a very good material quality. Room-temperature operated VCSELs exhibit around 0.5 mW of output power with singlemode-emission at 2.36  $\mu\text{m}$  representing the longest wavelength that has been achieved with InP-based interband lasers so far. GaSb-based devices comprise an epitaxial back mirror and a dielectric output mirror while the basic BTJ-principle is maintained. Using GaInAsSb quantum wells, the active region reveals excellent gain characteristics at 2.3  $\mu\text{m}$ . Singlemode VCSELs show room temperature threshold currents around 1 mA and output powers of 0.7 mW, respectively. Both laser types have been implemented in a tuneable diode laser spectroscopy (TDLS) setup to evaluate their capability for sensing of carbon monoxide. Using an absorption path length of only 10 cm, concentration measurements down to a few ppm have been successfully demonstrated.

**Keywords:** semiconductor laser, vertical cavity surface emitting laser, VCSEL, carbon monoxide, tunnel junction, InP, GaSb, absorption spectroscopy, optical sensing

## 1. INTRODUCTION

During the past two decades, vertical-cavity surface-emitting lasers (VCSELs) have been developed with a significant pace and are now among the most versatile semiconductor light sources for numerous applications. Compared to short-wavelength ( $<1 \mu\text{m}$ ) GaAs-based devices, the development of long-wavelength VCSELs with emission wavelengths beyond 1.3  $\mu\text{m}$  has been challenged by significantly more severe technological drawbacks. Due to innovative technological concepts, however, the performance of such devices has undergone a striking progress in recent years making these devices ideal light sources for a large number of applications particularly in optical communication and sensing.

Compared to conventionally used systems based on electrochemical point sensors, tuneable diode laser absorption spectroscopy (TDLS) offers tremendous benefits for the detection of gases such as rapid response time, long term stability, high selectivity and sensitivity, integral measurement capability over long distances using open path systems and sharply reduced maintenance efforts [1]. TDLS is based on the presence of strong absorption lines in the near- to mid-infrared spectral range. These molecule resonances cause characteristic "fingerprints" by selective absorption in the detector signal vs. laser operating current as the wavelength is tuned by changing the bias current.

The well known advantages of VCSELs such as longitudinal singlemode emission, small power consumption, superior beam quality and cost effectiveness particularly hold for TDLS applications in the long-wavelength range. Due to the smaller active volume, the current tuning rate is by a factor of 10-20 higher as compared to edge-emitting lasers.

\*ortsiefer@vertilas.com; phone 49 89 5484-2007; fax 49 89 5484-2019; www.vertilas.com

While interband transition DFB lasers on different material systems cover a detection range up to 3  $\mu\text{m}$  wavelength, the availability of VCSELs has been restricted to  $\sim 2 \mu\text{m}$  so far. The wavelength range between 2 and 3  $\mu\text{m}$ , however, comprises strong absorption lines of atmospheric pollutants or hazardous gases like CO, H<sub>2</sub>S, HF, CH<sub>4</sub>, CO<sub>2</sub> etc. These species are mainly used in applications for industrial process control, environmental and domestic air monitoring and safety surveillance.

In this paper we review the performance of long-wavelength VCSELs for emission wavelengths around 2.3  $\mu\text{m}$  and the results of absorption measurements of carbon monoxide (CO) at this wavelength. The latter one plays an essential role in a large variety of combustion processes and air monitoring tasks. CO is classified as a highly toxic gas and is usually generated by a partial oxidation of carbon containing combustibles. CO escaping from home burners is the most frequent cause for unintentional death at home with a death toll of annually 500 persons in the USA [2]. Moreover, it is the most prominent gas to be detected for gas sensor based fire detection.

In principal, two active region materials are possible for reaching emission wavelength around 2.3  $\mu\text{m}$ : highly strained GaInAs on InP and GaInAsSb on GaSb. The first approach includes the modification of the mature technology on InP thereby creating a reference for the recently fabricated devices based on GaSb. A comparison of both types as well as the device results and corresponding CO measurements are presented.

## 2. BURIED TUNNEL JUNCTION VCSELS BASED ON INP

For some years InP-based VCSELs with emission wavelengths ranging from 1.3 to 2.0  $\mu\text{m}$  have been fabricated by VERTILAS using the mature buried tunnel junction (BTJ) technology [3]. The design of InP-based VCSELs comprises a buried tunnel junction for self adjusted optical and current confinement, a bottom dielectric back mirror and integrated heatsink for reduced thermal resistance and an epitaxial top output mirror as depicted in Fig. 1. To expand this wavelength range to the desired new wavelength around 2.3  $\mu\text{m}$ , integral parts of the device like mirror composition and layer thicknesses can be adjusted in a straightforward manner.

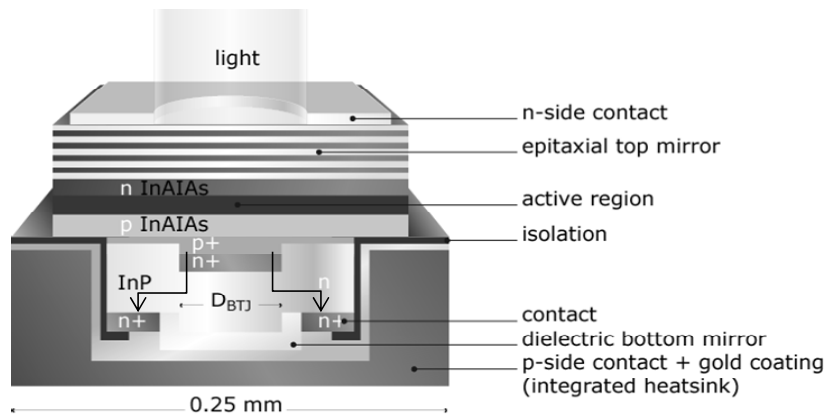


Figure 1. Schematic cross section of InP-based BTJ-VCSEL for sensing applications. The arrows indicate the locally restricted current flow through the tunnel junction.

For the active region, however, a new development became necessary since the strain of conventional rectangular quantum wells with homogeneous composition would exceed the critical limit already beyond an active region emission wavelength of  $\sim 2.05 \mu\text{m}$ . However, theoretical bandgap calculations show that the emission wavelength of a quantum well can be significantly increased if the standard rectangular shape of the indium content within the quantum well is changed to a triangular (V-shaped) one while keeping the average strain constant. An increasing amount of indium in the center of a symmetrical quantum well reduces the emission energy efficiently and therefore leads to a longer wavelength. The quantum wells are realized with a linear gradient in indium content between lattice matched GaInAs and pure InAs by using a digital alloy [4]. Fig. 2 shows the realized V-shaped quantum well starting with lattice-matched GaInAs after the tensile strained barrier followed by an increasing indium content every nanometer accomplished by opening and closing the gallium shutter and ending in the center with 1 nm pure InAs. This distribution of indium content and strain within the quantum well avoids direct interfaces between heavily tensile and compressive strained layers. Furthermore,

with the relieve of strain on the interface between barrier and quantum well it becomes possible to implement considerable tensile strain in the (Al)GaInAs barriers to partially compensate the compressive strain in the quantum wells. In addition, surrounding confinement layers are grown tensile strained to provide a pre-strained region in growth direction underneath the quantum wells and realizing above an almost balanced overall strain for the active region. The relevant growth parameters such as temperature and V/III ratio have to be adjusted to grow quantum wells and barriers with high crystalline quality. With these optimized growth conditions, VCSEL active regions comprising V-shaped quantum wells and tensile strained barriers have been successfully realized. A smooth surface morphology and a very detailed X-ray diffraction pattern including a perfect matching to the simulated nominal structure as shown in Fig. 2 give evidence that the multilayer structure can be grown perfectly pseudomorphic. Typically, the room temperature photoluminescence peak is detected around 2250 nm.

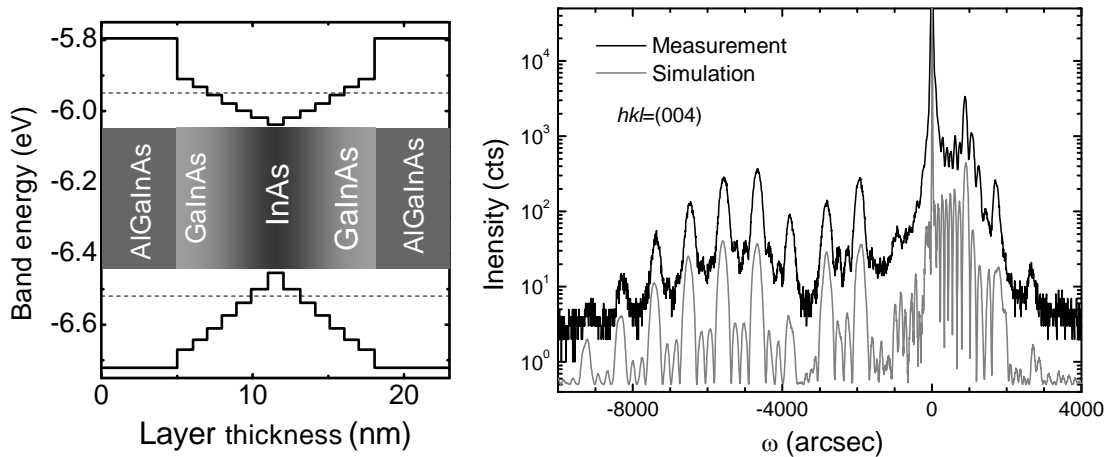


Figure 2. (a) Band structure of V-shaped quantum well. (b) X-ray diffraction pattern of a four QW active region.

The epitaxial front and dielectric back mirror of BTJ-VCSELs incorporating this new active region are made of 30.5 pairs of InGaAs/InAlAs and 2.5 pairs of CaF<sub>2</sub>/a-Si, respectively. The amorphous silicon allows for a high refractive index and small absorption at 2.3  $\mu$ m wavelength. Fig. 3 presents the light-current-voltage (*LIV*) characteristics and optical spectrum under continuous wave (cw) operation at room temperature.

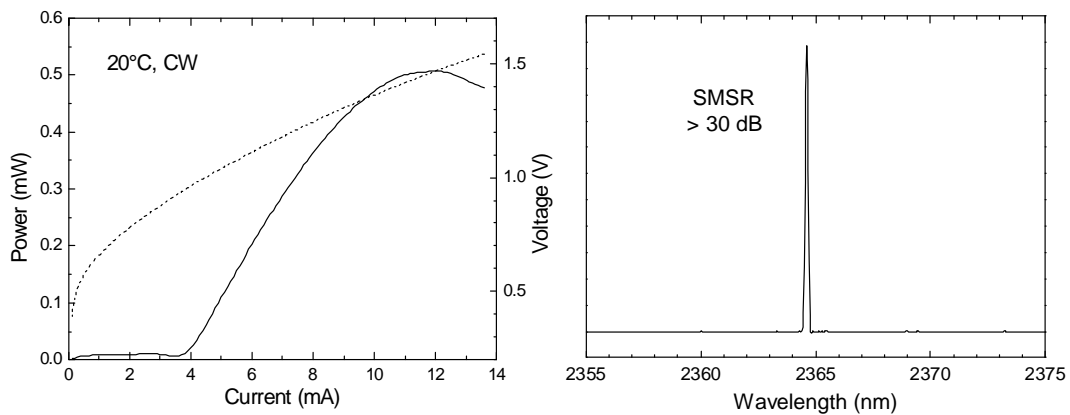


Figure 3. *LIV*-characteristics of InP-based 2.36  $\mu$ m BTJ-VCSEL with 6  $\mu$ m aperture diameter and corresponding emission spectrum.

Singlemode VCSELs with BTJ-diameters of 6  $\mu$ m show room temperature output powers up to 0.5 mW with a threshold current and voltage of 3.8 mA and 0.95 V, respectively. VCSELs with apertures of 12  $\mu$ m exhibit multimode output powers in excess of 1 mW. The maximum temperature for cw operation is detected around 60°C. Comparing the

threshold currents to BTJ-VCSELS at shorter wavelengths gives an increase by a factor of 2-4 which is mainly due to smaller gain performance, increased mode-gain offset of more than 100 nm as well as stronger losses like Auger recombination, free-carrier and intervalence band absorption. It should be noted that with an emission wavelength of more than 2.36  $\mu\text{m}$ , these lasers exhibit the longest wavelength for any InP-based interband transition diode lasers presented so far [5].

### 3. BURIED TUNNEL JUNCTION VCSELS BASED ON GASB

While wavelengths around 2.3  $\mu\text{m}$  undoubtedly mark a strict limit for InP-based diode lasers, the wavelength range between 2 and 3.3  $\mu\text{m}$  clearly favours material systems based on GaSb substrates. In recent years, impressive performance results have been obtained for edge emitters revealing excellent gain characteristics of GaSb-based active regions and also significant progress in corresponding VCSEL technology has been reported [6-8].

The device structure of the GaSb-based BTJ-VCSEL is shown in Fig. 4. As for its InP-based counterparts, the growth of the epitaxial laser structure is divided into two runs both performed by molecular beam epitaxy (MBE). In the first step, the epitaxial DBR consisting of  $\sim 24$  pairs of GaSb and AlAsSb quarterwave layers doped with tellurium, the active region and the tunnel junction are deposited. The active region is usually formed by compressively strained GaInAsSb quantum wells separated by AlGaAsSb barrier material. The tunnel junction layers are composed of  $p^+$ -GaSb and  $n^+$ -InAsSb. Due to its amphoteric behavior, silicon acts as a donor in InAsSb and as an acceptor in GaSb and thus can be used as dopant on both sides of the tunnel junction forming a low-resistive intra-device contact structure [9]. After the first epitaxial run, the tunnel junction is laterally dry-etched and overgrown with  $n$ -doped GaSb in the subsequent MBE growth step. As well known from the proven InP-based buried tunnel junctions, the GaSb-based structured tunnel junction likewise enables efficient current confinement and allows the substitution of  $p$ -doped layers by  $n$ -doped material with reduced electrical and optical loss. On top of the BTJ and below the active region,  $n$ -type GaSb current- and heat-spreading layers are located to reduce ohmic losses and to improve heatsinking. To complete the VCSEL-cavity, a dielectric output DBR consisting of 3 pairs of  $\text{SiO}_2/a\text{-Si}$  is deposited on top of the structure.

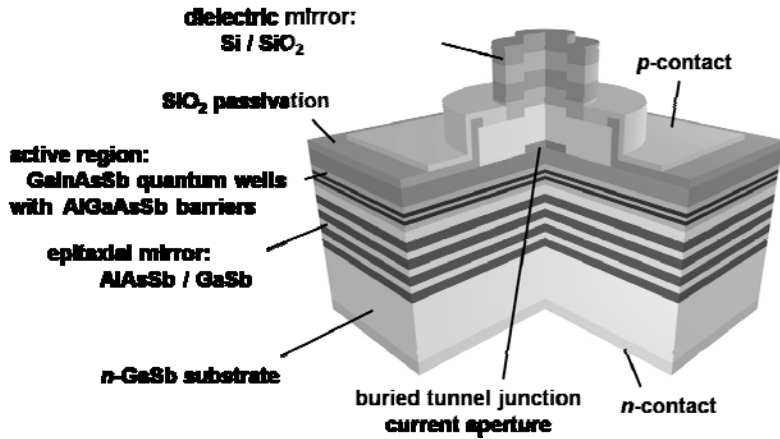


Figure 4. Schematic cross section of GaSb-based BTJ-VCSEL

The  $LI$  characteristics of a device with an elliptic aperture of  $6.4 \mu\text{m} \times 5.6 \mu\text{m}$  are shown in Fig. 5a. The maximum temperature for cw operation is as high as 90°C. At 0°C, the maximum output power is 0.8 mW and the threshold current is 1.2 mA corresponding to an effective threshold current density of only  $1.5 \text{ kAcm}^{-2}$  if a lateral diffusion of carriers of 2  $\mu\text{m}$  on each side is taken into account. For the presented devices, a continuous increase of threshold current is observed for temperatures between 0°C and 90°C. Since the VCSEL threshold current dependence on temperature is predominantly determined by the mode-gain offset, significant potential is expected for further device improvement regarding output power and maximum operating temperature by optimizing the relative alignment between gain maximum and cavity resonance. Fig. 5b shows the optical spectrum at different driving currents at a constant heatsink

temperature of 20°C. Devices with the aforementioned aperture size exhibit singlemode operation with a side-mode suppression ratio (SMSR) exceeding 25 dB. By electrothermal tuning, the emission wavelength tunes over a range of 10 nm (2348 nm to 2358 nm) yielding a tuning rate of 1.03 nm / mA. Together with a thermal tuning coefficient of 0.24 nmK<sup>-1</sup>, the VCSELs can be tuned over 20 nm in a temperature range from 0°C to 80°C.

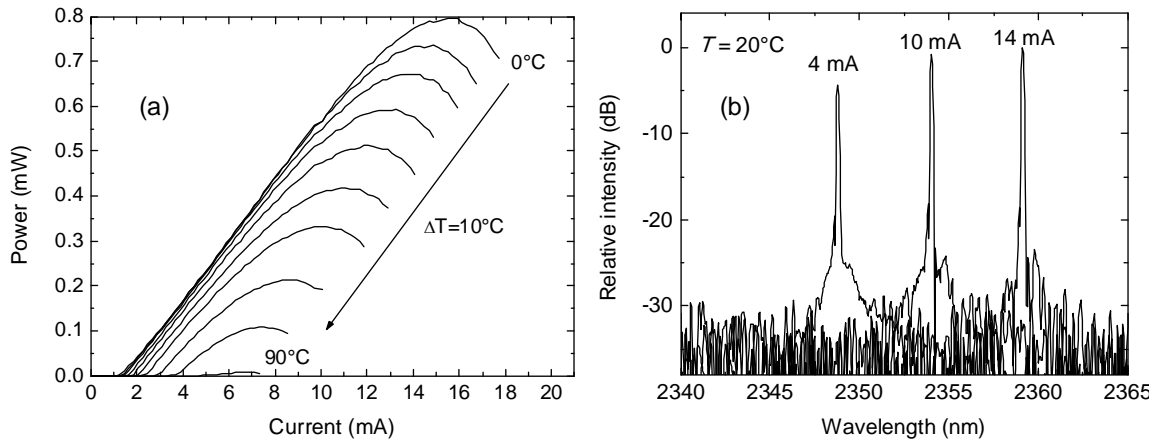


Figure 5. (a) Temperature dependent *LI*-measurements. (b) Spectra at different driving currents of 2.35  $\mu\text{m}$  GaSb-based BTJ-VCSEL.

#### 4. CARBON MONOXIDE ABSORPTION MEASUREMENTS

Fig. 6 shows the compact design of the sensor used for CO measurements. A spherical mirror is used to focus the light on the detector and to extend the absorption path length to 10 cm. A compact, microcontroller-based electronics unit serves as sensor control, signal processing and data evaluation. The current of the laser device is tuned periodically to scan the absorption spectrum while the temperature of the laser chip is kept constant by a controlled Thermo-Electric Cooler (TEC). For reliable measurements of trace gas concentrations with TDLS, precise knowledge of the absolute wavelength is mandatory. With CO being a trace gas in ambient air, the measured gas absorption spectrum provides no reliable indication of the CO absorption line position. Furthermore, the VCSEL current to wavelength relationship and its dependency on modulation frequency cannot be assumed to be constant for long-term sensor operation. For this reason, using a beam splitter and passing the laser beam parallel to the main cell through a reference cell which contains the gas in high concentration is often used for exact line locking [10]. To reduce the complexity of the optical system compared to such configurations, the current setup uses methane (CH<sub>4</sub>) in the photodetector housing, i.e. in the optical path of the absorption cell. A well defined methane absorbance of  $2.5 \times 10^{-3}$  is accomplished by filling the photodetector housing with 10% methane forming an optical absorption path of about 0.6 mm [11].

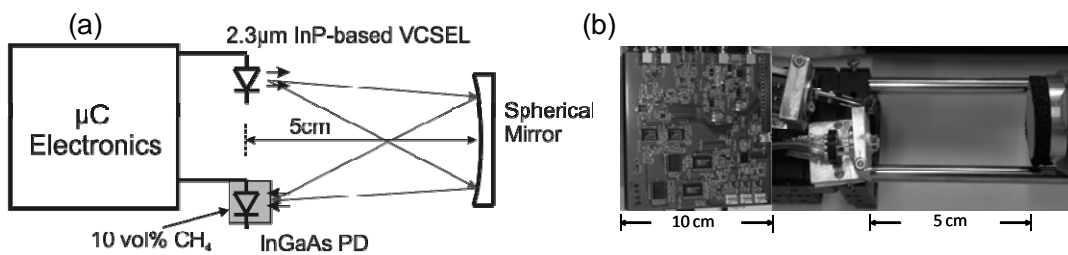


Figure 6. (a) Schematic measurement setup. (b) Image of final system including tuneable light source, GaInAs photo detector and free optical path (10 cm). The photo detector is filled with 10% methane enabling an auto-calibrating of the set-up.

For the absorption measurement, a wavelength range from 2364 to 2367 nm is selected as it comprises distinct CH<sub>4</sub> and CO lines within a reasonable tuning range. To achieve the desired wavelength, the heatsinks of both lasers types were adjusted. The emission wavelength of the InP-based VCSEL is already close to the desired wavelength range; therefore the heatsink temperature was only slightly increased to 33°C. For the GaSb-based VCSEL, a heat sink temperature of

82°C was necessary. The maximum output power at this temperature is reduced to  $\sim 100 \mu\text{W}$ . The wavelength scan is performed by changing the laser current, for the InP-based device from 8.5 to 11 mA and for the GaSb-VCSEL from 4.8 to 8 mA. Fig. 7 shows the second harmonic spectra recorded with both types of VCSELs.

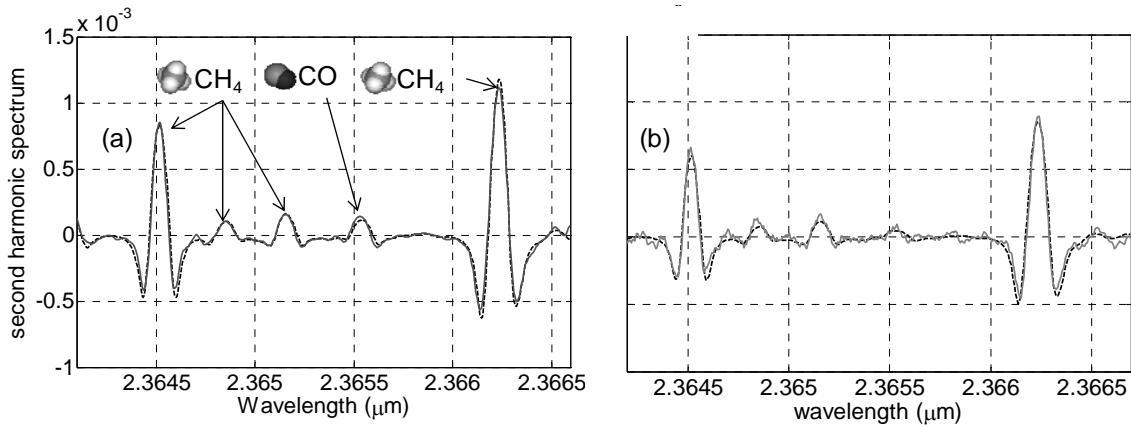


Figure 7. Second-harmonic spectra of a wavelength scan of (a) InP-based VCSEL (heatsink temperature 33°C, current: 8.5 to 11 mA). (b) GaSb-based VCSEL (heatsink temperature 82°C, 4.8 to 8 mA). Solid lines: measurement, dashed lines: fit

A wide scan as seen in Fig. 7a and 7b of about 3 nm every few seconds is used to identify the wavelength scale while a more frequent narrow scan of 0.7 nm in 0.1 s is performed to determine the CO concentration. The narrow scan is used with respect to improved bandwidth efficiency since it takes less time than the wide scan with the same signal to noise ratio. The wide scan involves at least three gas absorption lines (either  $\text{CH}_4$  and/or  $\text{CO}$ ) that are used to determine the linear and quadratic current to wavelength tuning coefficients. The quadratic term is necessary for precise determination of the wavelength scale which is needed for computation of the reference spectra for the narrow scan. On the other hand, the narrow scan applies a non-iterative linear least squares curve fit with the analytically computed reference spectra of  $\text{CO}$  and  $\text{CH}_4$  absorption lines by using the Lorentz line shape model [12] and the line parameters from the HITRAN database. Neither background or reference spectra measurements nor further calibration factors except for the line parameters from the HITRAN database and the gain of the second harmonic signal path of the sensor electronics are required. The relative intensity change of the detector signal with this method is about  $1 \times 10^{-5}$ . The concentration resolution of the  $\text{CO}$  sensor equipped with the GaSb-VCSEL is 4 ppm, which is slightly below the limit achieved by the  $\text{CO}$  sensor with the InP-based VCSEL of around 3 ppm.

## 5. CONCLUSION

We have realized extended wavelength VCSELs around 2.3  $\mu\text{m}$  emission on GaSb and InP-based materials. Both VCSEL types exploit the concept of buried tunnel junctions in conjunction with measures for improved heatsinking and can be conveniently operated in cw mode at room temperature or even beyond. While InP-based VCSELs at 2.3  $\mu\text{m}$  exhibit performance values inferior to their shorter counterparts and constitute a strict limitation for this material system, the initial results of GaSb-based VCSELs already show excellent threshold currents and operating temperatures. With future optimizations, it is expected to achieve even better output characteristics and to expand the VCSEL wavelength range at least up to 3  $\mu\text{m}$ .

With these devices, the first 2.3  $\mu\text{m}$  VCSEL-based  $\text{CO}$  sensor using a compact absorption cell capable of detecting  $\text{CO}$  with ppm resolution has been realized. By using the photodetector housing as a methane reference cell, a complicated measurement setup with a separate reference cell for line locking is dispensable. Distinctive long term stability can be expected as besides molecule parameters no further calibration factors are required. The setup allows for  $\text{CO}$  concentration measurements down to a few ppm.

## ACKNOWLEDGMENTS

This work has been supported by the European Union via NEMIS (contract no. FP6-2005-IST-5-031845), the German Federal Ministry of Education and Research via NOSE (contract no. 13N8772) and the Excellence Cluster "Nanosystems Initiative Munich (NIM)".

## REFERENCES

- [1] P. Werle, *Spectrochim. Acta Part A*, 54, 197 (1998).
- [2] Center for Disease Control and Prevention, Carbon Monoxide Poisoning: Fact Sheet. Online electronic publication: <http://www.cdc.gov/co/pdfs/faqs.htm> (2010).
- [3] R. Shau, M. Ortsiefer, J. Roskopf, G. Böhm, C. Lauer, M. Maute, and M.-C. Amann: "Long-wavelength InP-based VCSELs with Buried Tunnel Junction: Properties and Applications", *Vertical-Cavity Surface-Emitting Lasers VIII*, Proc. SPIE 5364, 1-15 (2004).
- [4] M. Ortsiefer, G. Böhm, M. Grau, K. Windhorn, E. Rönneberg, J. Roskopf, R. Shau, O. Dier, and M.-C. Amann, "Electrically pumped room temperature CW VCSELs with 2.3  $\mu\text{m}$  emission wavelength", *Electron. Lett.* 42, 640-641 (2006).
- [5] T. Sato, M. Mitsuhashi, N. Nunoya, T. Fujisawa, K. Kasaya, F. Kano, Y. Kondo, "2.33- $\mu\text{m}$ -Wavelength Distributed Feedback Lasers With InAs-In<sub>0.53</sub>Ga<sub>0.47</sub>As Multiple-Quantum Wells on InP Substrates", *IEEE Photon. Technol. Lett.* 20, 1045-1047 (2008).
- [6] C. Lin, M. Grau, O. Dier, M.-C. Amann, "Low threshold room-temperature continuous-wave operation of 2.24-3.04  $\mu\text{m}$  GaInAsSb/AlGaAsSb quantum-well lasers", *Appl. Phys. Lett.* 84, 5088-5090 (2004).
- [7] L. Shterengas, G. Belenky, T. Hosoda, G. Kipshidze, S. Suchalkin, "Continuous wave operation of diode lasers at 3.36  $\mu\text{m}$  at 12 °C", *Appl. Phys. Lett.* 93, (2008).
- [8] A. Ducanhez, L. Cerutti, A. Gassenq, P. Grech, F. Genty, "Fabrication and Characterization of GaSb-Based Monolithic Resonant-Cavity Light-Emitting Diodes Emitting Around 2.3  $\mu\text{m}$  and Including a Tunnel Junction", *IEEE J. Sel. Top. Quantum Electron.*, 1014-1021 (2008).
- [9] O. Dier, C. Lauer, M.-C. Amann, "*n*-InAsSb/*p*-GaSb tunnel junctions with extremely low resistivity", *Electron. Lett.* 42, 419-420 (2006).
- [10] H. Teichert, T. Fernholz, V. Ebert, "Simultaneous In Situ Measurement of CO, H<sub>2</sub>O, and Gas Temperatures in a Full-Sized Coal-Fired Power Plant by Near-Infrared Diode Lasers", *Appl. Opt.* 42, 2043-2051 (2003).
- [11] A. Hangauer, J. Chen, R. Strzoda, M. Ortsiefer, M.-C. Amann, "Wavelength modulation spectroscopy with widely tunable InP-based 2.3  $\mu\text{m}$  vertical-cavity surface-emitting laser", *Opt. Lett.* 33, 1566-1568 (2008).
- [12] R. Arndt, "Analytical Line Shapes for Lorentzian Signals Broadened by Modulation", *J. Appl. Phys.* 36, 2522 (1965).